

## Diverse Classical Walking of a Single Atom in an Amplitude-Modulated Standing Wave Lattice

Lin Zhang,\* H. Y. Kong, and S. X. Qu

*Institute of Theoretical and Computational Physics,  
Shaanxi Normal University, Xi'an 710062, P. R. China*  
(Received July 22, 2010)

The classical walking behavior of a single atom in an amplitude-modulated standing wave lattice is investigated. Based on a simple effective model, we identify a diversity of dynamical regimes of atomic motion by periodically adjusting the lattice depth. Harmonic oscillation or pendulum rotation with classical step-jumping, random scattering walking, chaotic transportation, quasi-periodic trapped motion, and roughly ballistic free flying are found in this simple model within different parametric regions. Our study demonstrates a complex motion of single atom in a modulating optical lattice beyond the quantum description.

PACS numbers: 05.45.Mt, 37.10.Jk, 05.40.-a, 37.10.Vz

### I. INTRODUCTION

Nowadays, fabrication technology steps more and more towards the atomic scale, and the detection of one single molecule or atom is now a promising technique [1, 2]. Controlling one atom in cavity quantum electrodynamics has now nearly met this step [3–5]. Based on optical techniques, the motion of one single atom in a controlled 1-dimensional (1D) optical lattice becomes a hot topic with continuous interests for its basic theoretical value and potential applications in quantum information processing [6], atomic lithography [7], solid state physics [8], quantum walking algorithm [9, 10], plasmonic application [11, 12], quantum-to-classical transition [13], and molecular dynamics. In an optical lattice, the atom can be accelerated [14] or decelerated [15] by an optical force for the purpose of precise control. However, on the atomic scale, quantum effects start to play a tricky role in atomic dynamics. For example, under a deterministic linear force, the atomic motion is still beyond definite prediction in quantum theory because of an intrinsic uncertain fluctuation. That a quantum motion is distinguished from a classical trajectory motion is actually due to the superposition of the atomic wave packet, which induces interference effects such as dynamical localization [16]. But, just for one single atom, the external wave superposition will be excluded [17] and the motion at different times also will not interfere, unless a long memory imprinted on the optical field can feed back to the atomic motion along the classical trajectory. However this memory will be cut down by a definite external optical control. Therefore the quantum motion and the classical motion meet at this single atomic scale.

According to the quantum descriptions, by including the internal quantum transitions, many kinds of motional behavior were found for this single atomic system, such as

nonclassical motional states, ballistic transport, harmonic oscillations, random walks, Lévy flights, and chaotic transport [18–23]. Which of these behaviors are derived from the quantum description and which come from classical dynamics are still unsolved problems in this system. This multiple dynamics inspires us to find if there exists a simple classical model without internal dynamics which can reproduce most of the above dynamical processes. The interesting thing is that, in this paper, we do find a simple classical model which can produce most of above behaviors without directly considering internal dynamics. We identify a rich dynamical picture of the atomic motion in this classical model in order to pick up all the classical information from a mixture of descriptions. Our study is not trying to give the differences between the quantum dynamics and classical dynamics, because the different descriptions will definitely give different results, such as using different phase-space distribution functions [24]. The only thing to do, in this paper, is to find out all the classical dynamics of atomic walking within a classical framework and make an attempt to show whether some nonclassical motions are more a classical collective behavior (or a long time statistical behavior) than a quantum wave description of an individual particle. In order to give a full picture of the classical motion for a quantum system that is easy to check, we closely investigate the classical walking of a single atom in a controlled optical lattice. We first derive the simple classical dynamics model in Section II, and find a variety of atomic walking behaviors of the model in Section III. Some approximate analytical solutions in specific conditions are given to reveal the complicated behavior of atomic walking in this unsolvable model. Section IV provides a simple discussion and the main conclusions.

## II. THE SIMPLE CLASSICAL MODEL

What we start with is a widely verified quantum model which describes the dipole interaction between an atom and a classical field named the Rabi model [25]. The dynamics of a two-level atom with a dipole moment  $\mathbf{d}$  interacting with a quasi-monochromatic plane-wave field,

$$\mathbf{E}(\mathbf{r}, t) = \mathbf{e}_\lambda \mathcal{E}(\mathbf{r}, t) \cos(\nu t - \mathbf{k} \cdot \mathbf{r}), \quad (1)$$

is described by the Hamiltonian

$$\hat{H} = \frac{\hat{\mathbf{p}}^2}{2m} + \frac{1}{2} \hbar \omega_0 \hat{\sigma}_z - \hbar \Omega(\mathbf{r}, t) \cos(\nu t - \mathbf{k} \cdot \mathbf{r}) (\hat{\sigma}^- + \hat{\sigma}^+), \quad (2)$$

where the Rabi frequency is defined by  $\Omega(\mathbf{r}, t) = \mathcal{E}(\mathbf{r}, t) \cdot \mathbf{d} / \hbar$ . In Eq. (1),  $\mathcal{E}(\mathbf{r}, t)$  is the temporal envelope of the wave field which can be definitely controlled in the experiment. The modulated Rabi frequency  $\Omega(\mathbf{r}, t)$  expresses the coupling intensity of the field mode with the atomic dipole  $\mathbf{d}$ , and  $\hat{\sigma}^+$  ( $\hat{\sigma}^-$ ) is the atomic level raising (lowering) operator. The Hamiltonian (2) is a widely used model for studying the interaction between a two-level atom and a classical field with different controlling modes denoted by  $\Omega(\mathbf{r}, t)$ .

However, what we consider here is a simple case: a single atom interacts with a standing wave mode in a microcavity with only its axial direction,  $x$ , getting involved. In

this case, the Hamiltonian becomes

$$\hat{H} = \frac{\hat{p}^2}{2m} + \frac{1}{2}\hbar\omega_0\hat{\sigma}_z - \hbar\Omega(x, t)\cos\nu t(\hat{\sigma}^- + \hat{\sigma}^+), \quad (3)$$

where  $\Omega(x, t)$  depends on the axial cavity mode with an envelope modulated by the input field. In a resonant mode field, Eq. (3) reduces to a so-called double resonance model [26] with an effective Hamiltonian of (see Appendix A for details)

$$\hat{H} = \frac{\hat{p}^2}{2m} - \hbar\lambda\cos(\chi t)\cos(k\hat{x}), \quad (4)$$

where the key parameter  $\chi$  is the modulation frequency of the field amplitude. Eq. (4) is an extensively considered model [27–30] along with the phase-modulated model [31] in quantum chaos. Here the Hamiltonian describes the dynamics of an atom (or a polar molecule) moving in an amplitude-modulated standing wave under an effective coupling constant  $\lambda$ . However in quantum theory, this model is time-dependent and difficult to solve using normal techniques [32]. For one single atom, we can introduce the following dimensionless classical variables  $H = \langle \hat{H} \rangle / \hbar\omega_r$ ,  $p = \langle \hat{p} \rangle / \hbar k$ ,  $x = k\langle \hat{x} \rangle$ , and dimensionless parameters  $\lambda' = \lambda/\omega_r$ ,  $\omega = \chi/\omega_r$ ,  $t' = \omega_r t$ , scaled by the recoil frequency of a single photon  $\omega_r = \hbar k^2/m$ . The label  $\langle \hat{O} \rangle = O$  means the expectation value of the corresponding quantum operator  $\hat{O}$ , and this is a very good approximation for one single atom in a good cavity. On the atomic scale, a single atom can be treated as a classical point with its position identified by the center of mass, and no fluctuations induced by spatial superposition exist here. Therefore the classical model can be obtained (primes are omitted) as

$$H(t) = \frac{p^2}{2} - \lambda\cos x\cos\omega t. \quad (5)$$

According to Eq. (5), the classical dynamic equations are

$$\dot{x} = \frac{\partial H}{\partial p} = p, \quad \dot{p} = -\frac{\partial H}{\partial x} = -\lambda\sin x\cos\omega t, \quad (6)$$

or

$$\ddot{x} + \lambda\cos\omega t\sin x = 0. \quad (7)$$

Eq. (7) looks simple, but it is an amplitude-modulated pendulum equation and no closed analytical solution for an arbitrary parameter is available [33].

The steady solutions of Eq. (7) are clear at the antinode sites for  $x^* = 0, \pm\pi, \pm 2\pi, \dots$  and  $p^* = 0$ , but they are not always stable because the trapping potential is time-dependent with the form

$$V(x, t) = -\lambda\cos(\omega t)\cos x = -\frac{\lambda}{2}[\cos(x + \omega t) + \cos(x - \omega t)],$$

which acts on the atom as a superposition of two potential waves propagating in opposite directions. In a high finesse cavity, this potential is usually used to control the atomic

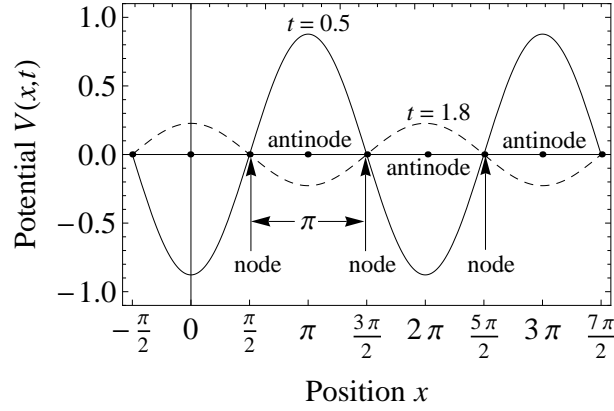


FIG. 1: The effective potential along lattice  $x$  at different times,  $t = 0.5$  (solid line) and  $t = 1.8$  (dashed line), with parameters  $\lambda = 1$ ,  $\omega = 1$ . The time  $t$  is scaled by the recoil frequency  $\omega_r$  and the position  $x$  is scaled by the wavelength of the cavity mode.

motion and can be easily generated by a modulation of the standing cavity-mode. Fig. 1 shows the varying potentials at two different times along the axial direction. The nodes (indicated by arrows) or antinodes of the potential lattice are fixed with a spatial period of  $\pi$  but the amplitude of the lattice wave changes with time with a period of  $t = 2\pi/\omega$ . The amplitude  $\lambda$  at the antinodes denotes the atom-lattice coupling indicating a trapping ability of the atom at an antinode, so we can call it a lattice depth. All of the above lattice parameters can influence the dynamics of the atom, and all can be controlled by an external optical field.

However, due to the atomic motion, the potential lattice felt by the atom also depends on the momentum of the atom. If we suppose that the velocity of the atom is a slowly varying quantity during a time period of  $[0, t]$ , we can set

$$x(t) = \int_0^t p(\tau) d\tau = \langle p \rangle \cdot t \approx p_0 \cdot t,$$

where  $\langle p \rangle$  is a time average of the momentum which can be replaced by its initial value of  $p_0$ . In this case, the optical force will be

$$F(t) = -\frac{\partial V}{\partial x} = -\frac{\lambda}{2} [\sin(\omega + p_0)t - \sin(\omega - p_0)t], \quad (8)$$

which clearly indicates that there are two driven forces exerted on the atom with two different frequencies depending on the atomic momentum, suggesting two nonlinear resonance points of the dynamics at  $\omega \pm p_0$  [26]. Therefore, the motion of the atom across the varying lattice field is dependent on two aspects: the lattice field and the state of the atom. Although this model described by Eq. (5) is simple, it can display most of the dynamic behaviors found in [19–23] without directly including the internal dynamics.

### III. DIVERSITY OF WALKING BEHAVIOR

#### III-1. Oscillation with random step-jumping

Under the condition that the amplitude of the lattice is varying slowly, the cold atom ( $p < 2\sqrt{\lambda}$ ) will be trapped at the bottom of the lattice potential for a long time, oscillating around the antinodes at  $\sin x^* = 0$ , i.e.,  $x^* = \pm n\pi, n = 0, 1, 2 \dots$ . In Fig. 2, a typical walking process of this case is shown by a numerical simulation of Eq. (6). Fig. 2(a) displays a temporal position (black line) and momentum (gray line) of the atomic walking, and Fig. 2(b) is its orbit in the phase space. We can see that the atom first oscillates

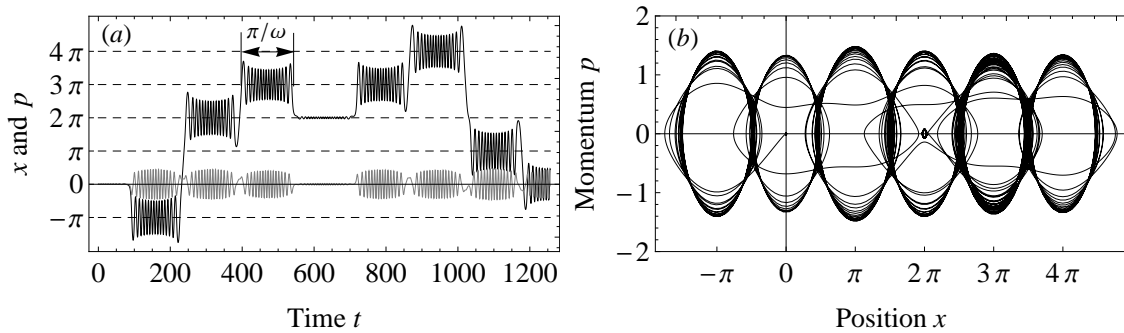


FIG. 2: A typical walking trajectory of a cold atom in a slowly varying standing wave with  $\lambda = 1$ ,  $\omega = 0.02$ ; the initial position and momentum are  $x_0 = 0$ ,  $p_0 = 0.02$ . (a) The evolution of the atomic position (black line) and momentum (gray line). (b) The corresponding orbit in phase space.

around one of the antinodes (indicated by the horizontal dashed lines) and then jumps randomly in integer steps of  $\pi$  to a left or right antinode after a time interval of  $\pi/\omega$ . The random atomic jumping to a new site is due to the loss of stability of the former site when the coupling intensity  $\lambda(t) = \lambda \cos(\omega t)$  turns from positive to negative. This classical jumping behavior demonstrated in this model will reversely affect the lattice field and can be traced by the transmission field from the cavity due to a motion-dependent detuning effect [34, 35]. Although a similar dynamical behavior was revealed by Domokos and Ritsch [36], the mechanisms of the two systems are different. Our system is only for one single atom and no random Langevin-type noise is necessary during the dynamics. In order to understand more about this classical trapping and jumping behavior, we can analyze it by the following extreme approximations.

#### 1. Harmonic Oscillation with random jumping

For a small modulation frequency  $\omega \ll 1$ , the approximation of  $\cos \omega t \sim 1$  is valid for a short time. The linearization for a cold atom ( $p \ll \sqrt{\lambda}$  for tightly trapped) around the stable positions of  $\sin x^* = 0$ , such as  $\sin x \sim x$  around 0 (for another site we can set

$x' = x - x^*$ ) can be used here. Then Eq. (7) will reduce to

$$\ddot{x} + \lambda x \approx 0, \quad \omega \ll 1, \quad (9)$$

where we set  $\lambda > 0$ , and this enables for Eq. (9) a harmonic oscillation solution of

$$x(t) \approx x(0) \cos(\sqrt{\lambda}t) + \frac{p(0)}{\sqrt{\lambda}} \sin(\sqrt{\lambda}t), \quad (10)$$

which describes the main properties of atomic walking in this case. Eq. (10) indicates that the oscillation frequency in Fig. 2(a) is determined by the depth of the trap,  $\lambda$ , and gives an important characteristic time of the oscillation period,  $2\pi/\sqrt{\lambda}$ . As the temporal depth  $\lambda(t) = \lambda \cos \omega t$  changes slowly with time, the oscillation frequency will adiabatically follow with  $\sqrt{\lambda(t)}$ . When  $\lambda(t)$  becomes negative, the oscillation frequency  $\sqrt{\lambda(t)} \rightarrow i\sqrt{|\lambda(t)|}$ , and the atom will escape exponentially from the former site in the manner of

$$x(t) \approx x(0) \cosh(\sqrt{\lambda}t) + \frac{p(0)}{\sqrt{\lambda}} \sinh(\sqrt{\lambda}t). \quad (11)$$

Therefore the atom will conduct an oscillation followed by an escaping jump from the former site. In order to see the details of this motion, Fig. 3(a) exhibits a zoomed in orbit around

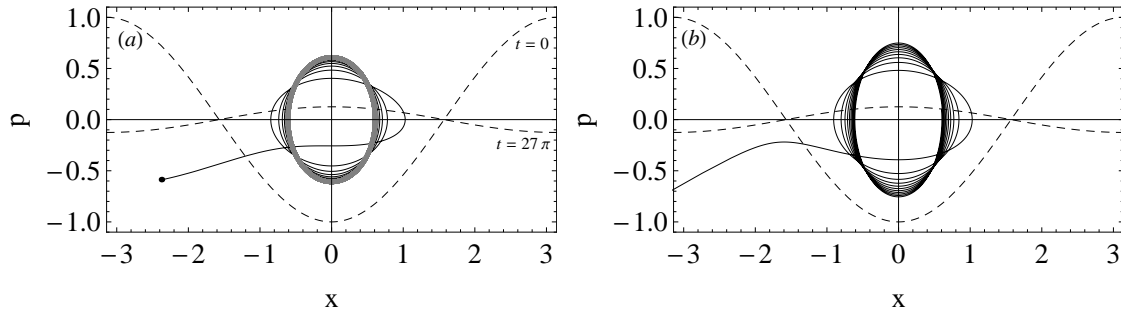


FIG. 3: The enlarged orbit of a cold atom in phase space with  $\omega = 0.02$  and  $\lambda = 1$ . The initial position and momentum are  $x_0 = 0.6$ ,  $p_0 = 0.1$ . (a) The orbit of the rigid simulation (solid black line) with harmonic approximation (gray thick line); (b) The approximation orbit of the Airy solution of Eq. (13).

one antinode in phase space. The black line is the real orbit and the thick gray ellipse stands for the harmonic oscillation of Eq. (10), where the potential lattices at time  $t = 0$  and at the end of one oscillation  $t = 27\pi$  are depicted by the dashed lines for reference. With a decrease of  $\lambda(t)$ , the elliptical orbit in the phase space expands along  $x$  until  $\lambda(t)$  decreases to a value that the atom can pass through it to another site at a location determined by the escaping momentum. Therefore the trapping time around antinodes for the cold atom is about  $\pi/\omega$  as indicated in Fig. 2(a), which is estimated as the time when  $\lambda(t)$  changes from a positive value to a negative value. In Fig. 3(a), the oscillating time of the atom

around the starting site is about  $t = \pi/2\omega = 25\pi$ , which is just the time taken by the trap depth  $\lambda(t)$  to decrease from maximum to zero.

Certainly, for a more rigorous approximation in above case of  $\omega t \ll 1$ , the time dependent part will be  $\cos(\omega t) \approx 1 - (\omega t)^2/2$ , and the atomic motion can be better described by a parabolic cylinder function satisfying the differential equation

$$\ddot{x} + \lambda\left(1 - \frac{\omega^2 t^2}{2}\right)x = 0, \quad (12)$$

or even by an Airy function determined by

$$\ddot{x} + \lambda\left(\frac{\pi}{2} - \omega t\right)x = 0, \quad (13)$$

where the time approximation  $\cos(\omega t) = \sin(\pi/2 - \omega t) \approx \pi/2 - \omega t$  is used. Fig. 3(b) demonstrates the improved orbit of the Airy solution compared to a harmonic oscillation in a short time. But for a longer time the dynamics will dramatically deviate from the real orbit because of the divergence of the Airy function.

## 2. Pendulum rotation with random step-shifting

When the varying frequency  $\omega$  increases nearly to the oscillation frequency  $\omega \sim \sqrt{\lambda}/2$ , the trapping time  $\pi/\omega$  of the cold atom will decrease, and the atom will quickly shift from one site to another like a pendulum swinging or rotating around different equilibrium sites just for a few periods. As the motion of the atom covers a large range of  $x$  relative to the stable antinodes in this case, the spatial linearized Eq. (9) will be invalid. Therefore Eq. (7) should be

$$\ddot{x} + \lambda \sin x = 0,$$

which is the well-known pendulum equation with  $\lambda > 0$ . Actually, this situation corresponds to an atom moving in a stationary one-dimensional lattice. When  $\lambda > 0$  the integral solution of the above equation takes the form of

$$x(t) = 2 \arcsin \left[ \sin \frac{x_0}{2} \operatorname{SN} \left( \sqrt{\lambda} t + K \left( \sin \frac{x_0}{2} \right), \sin \frac{x_0}{2} \right) \right], \quad (14)$$

with the initial conditions of  $x(0) = x_0$ ,  $\dot{x}(0) = 0$ . The label  $\operatorname{SN}(\cdot, \cdot)$  is the Jacobi elliptic function, and  $K(\cdot)$  is the complete elliptic integral of the first kind defined by the elliptic integral of

$$K(k) = \int_0^{\pi/2} \frac{d\theta}{\sqrt{1 - k^2 \sin^2 \theta}}.$$

Walking orbits in the optical lattice with a higher modulation frequency  $\omega = 0.1$  are demonstrated in Fig. 4. Fig. 4(a) is a rigid simulation, and Fig. 4(b) presents pendulum samples of a phase picture with random initial positions. We can see that the long-time

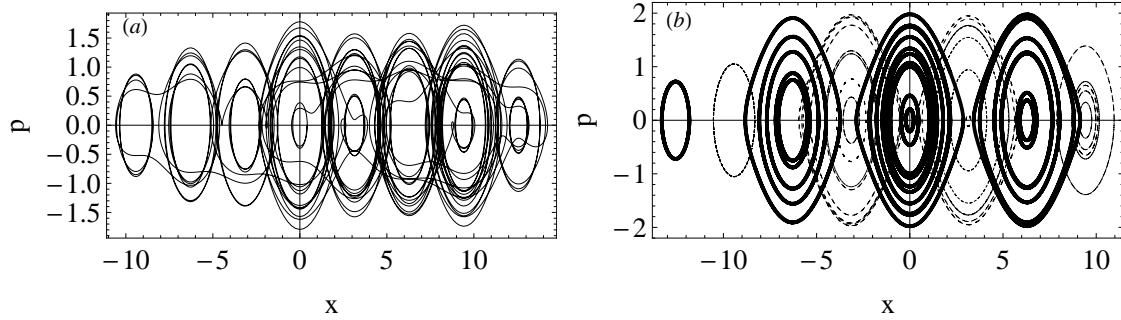


FIG. 4: The phase space picture of a cold atom walking in a slowly varying field with  $\lambda = 1$ ,  $\omega = 0.1$ , and the initial atomic momentum  $p(0) = 0$ . (a) The rigorous solution for the initial position is  $x(0) = 0.4$ ; (b) the pendulum solution of Eq. (14) by using a random step-shifting (step unit  $\pi$ ) position of a Gaussian distribution with a mean value of 0.4 and variance of  $\pi/2$ .

atomic walking can be somewhat (not exactly) explained by the pendulum solutions with random shifting equilibrium positions. As the effective  $\lambda(t)$  is actually time-dependent, the length of the pendulum will change gradually from positive to negative. When  $\lambda(t) < 0$ , the stable sites at  $x^* = 0, \pm 2\pi, \pm 4\pi, \dots$  for  $\lambda(t) > 0$  will become unstable and shift to new stable sites at  $x^* = \pm\pi, \pm 3\pi, \dots$ , which is clearly shown in Fig. 2(a) with a sequence of  $-\pi, 2\pi, 3\pi, 2\pi, 3\pi, 4\pi, \pi, 0\pi, \dots$ . In Fig. 4(b) the thick black lines are pendulum solutions of Eq. (14) for  $\lambda > 0$  and the thin dashed lines are for  $\lambda < 0$ . We use a Gaussian random number to pick up the initial positions for the pendulum samples, and the results reveal that a long time atomic walking in Fig. 4(a) can be illustrated by Eq. (14) with a random shifting of the equilibrium position of the pendulum rotation. The simulation indicates that this behavior is a combination of deterministic pendulum oscillation with a random shifting lattice.

According to the above analysis, we can conclude that, in a slowly modulated optical lattice, the cold atom will feel a gradually changing wave trap, resulting in a harmonic or pendulum rotation followed by a random step-shifting. In this process, two characteristic times are important, the trapping time  $\pi/\omega$  and the oscillation period  $2\pi/\sqrt{\lambda}$ . In addition, the step-shifting between antinodes of the lattice has a random characteristic and cannot be predicted, because the jumping process is very sensitive to position and momentum. In this respect, the atomic walking in a modulated standing wave is very similar to the one-dimensional billiard problem, in that a minor deviation of position (or momentum) will lead to a dramatically different walking orbit. However, the above conclusion is on the conditions that the optical lattice is slowly modulated and the atom is very cold. In the following parts we will find some other specific walking behaviors beyond these constraints.

### III-2. Random walking and Chaotic transportation

When the modulation frequency of the lattice is further increased, the trapping time of the cold atom,  $\pi/\omega$ , will decrease to an extent that it is comparable to the shifting time

between different sites,  $\pi/\langle p \rangle$  ( $\langle p \rangle$  is the average momentum during a walking interval). In this case, the atom will exhibit a random like walking that is shown in Fig. 5(a) by a

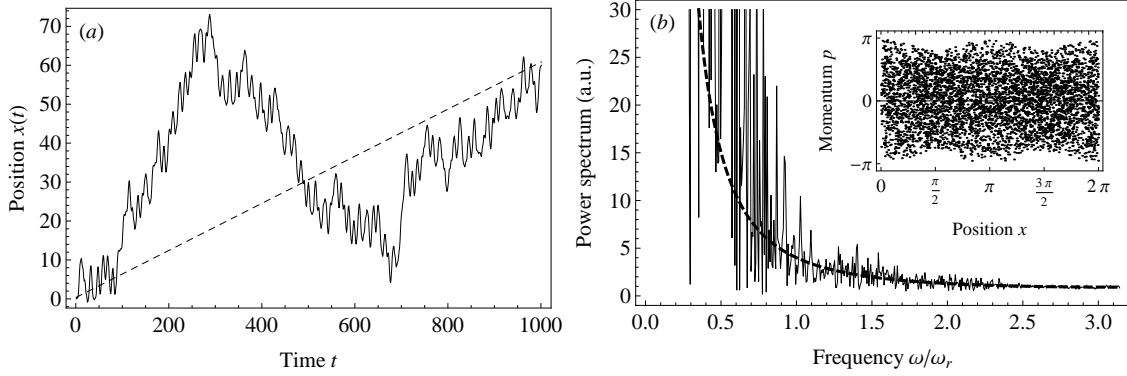


FIG. 5: (a) A typical random walking of a cold atom in a varying standing field of  $\omega = 0.8$ ,  $\lambda = 2$  with  $x(0) = 0$ ,  $p(0) = 0.4$ . The dashed line is the average motion of the atom. (b) The corresponding power spectrum of the random walking (solid) and the average motion (dashed). The inset picture is the phase-space distribution of the walking mapped to  $[0, 2\pi]$ .

typical sample of a moving sequence along the optical lattice, displaying an unpredictable position of the atom in the periodically varying lattice. This random characteristic can be further verified by a power spectrum of this walking depicted in Fig. 5(b). The dashed line in Fig. 5(a) corresponds to the effective uniform motion of this walking with an average momentum of  $\langle p(t) \rangle_T \approx 0.4 + 0.06$  ( $T$  is the total walking time), whose fourier spectrum is depicted by a thick dashed line for reference. The inset picture of Fig. 5(b) is a long time phase-space distribution of the atom by mapping its walking position into the first periodic region of the lattice  $[0, 2\pi]$ . The uniform phase-space distribution is a statistical proof of the random properties coming up in this deterministic system where regular and chaotic regions coexist in this walking process.

In the sense of walking sensitivity to the atomic state, the above behavior can be treated as a chaotic transportation in the standing wave lattice similar to the results in [19, 23]. The estimation of Lyapunov exponents  $\lambda_i$  can give a rough analysis of this chaotic property. This system is equivalent to a 3-dimensional autonomous system with one Lyapunov exponent being zero (the third dimension is  $\theta = \omega t$ ). Because the sum of the exponents for a Hamiltonian system is null, i.e.,  $\sum_i \lambda_i = 0$ , therefore the Lyapunov exponents of this system must be  $-r, 0, +r$ . Fig. 6 gives a rough estimate of the largest Lyapunov exponent  $r$  changing with the trapping depth  $\lambda$  (Fig. 6(a)) and with the modulation frequency  $\omega$  (Fig. 6(b)), indicating a weak chaotic transportation along the standing wave lattice. The chaotic transportation of this system under the influence of internal transitions has been investigated by Argonov and Prants [19, 20, 23], but our results reveal that only the external walking of an atom in a slowly varying optical lattice can present similar chaotic behavior. Certainly, the similar fractal tunneling time [37] through a lattice with a certain length can also be found in this walking.

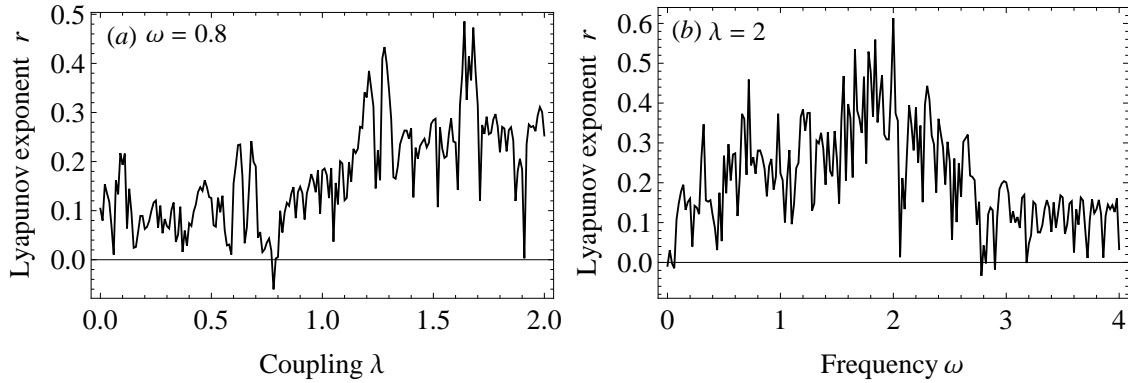


FIG. 6: (a) The Lyapunov exponent of the atomic walking versus coupling intensity  $\lambda$  with  $\omega = 0.8$ . (b) The Lyapunov exponent versus modulation frequency  $\omega$  with  $\lambda = 2$ . The initial atomic position is  $x(0) = 0$ , momentum  $p(0) = 0.4$ .

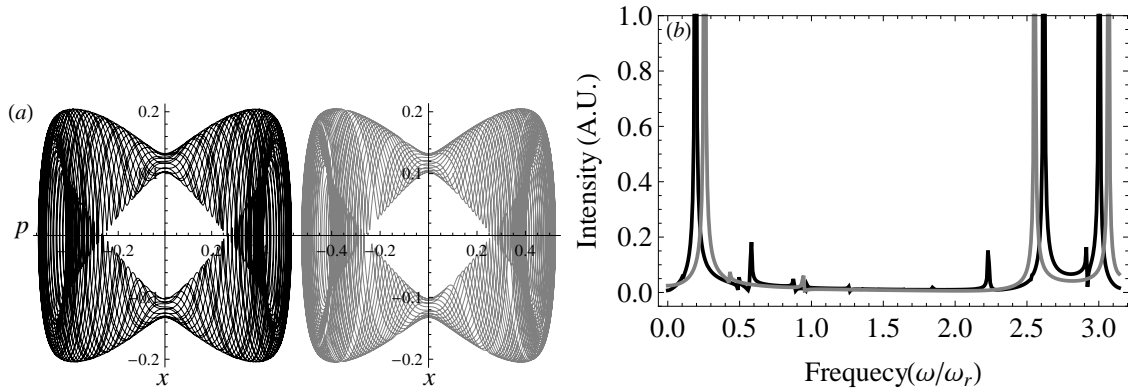


FIG. 7: (a) The phase portrait of a strict solution of Eq. (7) (left black orbit) and the Mathieu solution of Eq. (16) (right gray orbit) with parameters  $\lambda = 1$ ,  $\omega = 2.8$  and the initial position and momentum being  $x(0) = 0.2$ ,  $p(0) = 0.18$ . (b) The corresponding power spectrum of the atomic momentum for the strict solution (black line) and the Mathieu solution (gray line).

### III-3. Quasi-periodic trapping state and its stability

In some parametric regions the atom will be totally trapped by the quickly varying standing wave. Fig. 7(a) gives an example of this case when the frequency reaches to  $\omega = 2.8\omega_r$  (left black bowknot orbit). In this case the atom takes a periodic or quasi-periodic oscillation around a stable site near the initial position  $x(0)$ . In the following, we will give some detailed analysis about this trapped walking behavior.

For an arbitrary varying frequency  $\omega$ , Eq. (7) corresponds to a pendulum with changing length. The normal method of solving this nonlinear differential equation is the lineariza-

tion approach. For the trapped atom that is very near to a stable antinode of  $\sin x^* = 0$ , for example, a small  $x$  near zero has  $\sin x \sim x$ , Eq. (7) will be reduced to

$$\ddot{x} + (\lambda \cos \omega t) x = 0, \quad (15)$$

which is a linear equation with a periodic coefficient that can be solved by Floquet's theorem [38]. The linearized Equation (15) is a Mathieu equation,

$$\frac{d^2 x}{dt^2} + [a - 2q \cos(2t)] x = 0,$$

with a standard form of solution:

$$x(t) = e^{i\mu t} X(t),$$

where  $\mu$ , in general, is a complex function of  $a$  and  $q$  called the characteristic exponent, and  $X(t)$  is a periodic function. Explicitly, the solution of Equation (15) reads

$$x(t) = x(0)C\left(0, -\frac{2\lambda}{\omega^2}, \frac{\omega t}{2}\right) + p(0)S\left(0, -\frac{2\lambda}{\omega^2}, \frac{\omega t}{2}\right), \quad (16)$$

where  $C\left(0, -\frac{2\lambda}{\omega^2}, \frac{\omega t}{2}\right)$  and  $S\left(0, -\frac{2\lambda}{\omega^2}, \frac{\omega t}{2}\right)$  are Mathieu even and odd functions. The above solution can be used to estimate a variety of behaviors of Eq. (7) under the trapping condition (so that the linearization condition is valid). Fig. 7(a) is a comparison of the Mathieu solution (right gray orbit) with the strict simulation (left black orbit) in phase space when the Mathieu function is in its stable parametric region. The figures show a nice match of the linear approximation with Eq. (7) and the atom conducts a quasi-periodic oscillation around  $x^* = 0, \pm\pi, \pm2\pi, \dots$ . The quasi-periodic properties of this walking can be verified by the power spectrum of the atomic momentum in Fig. 7(b), where several frequency components are manifest but the atom never exactly repeats its walking orbit in the phase space. Certainly, for some parameters, periodic walking is also available. This can be discussed by using the characteristic exponent of the Mathieu function. The characteristic exponent,  $\mu(a, q) = \mu(0, -2\lambda/\omega^2)$ , predicts that only for certain values of  $\lambda$  and  $\omega$  can the solution be periodic. For parametric values of  $2\lambda/\omega^2 > 0.91$ ,  $\mu$  will be a complex number and Eq. (15) is unstable (see the borderlines  $2\lambda/\omega^2 \approx \pm 0.91$  shown in Fig. 8(a)). Therefore we can determine the stable or unstable parametric region of the linearization equation under independent initial conditions. However in a real system, the modulating amplitude will include a small constant part  $\mathcal{E}_0$  [39] that is governed by

$$\frac{d^2 x}{dt^2} + (\mathcal{E}_0 + \lambda \cos \omega t) x = 0,$$

and this enables a normal Mathieu solution of

$$x(t) = x(0)C\left(\frac{4\mathcal{E}_0}{\omega^2}, -\frac{2\lambda}{\omega^2}, \frac{\omega t}{2}\right) + p(0)S\left(\frac{4\mathcal{E}_0}{\omega^2}, -\frac{2\lambda}{\omega^2}, \frac{\omega t}{2}\right). \quad (17)$$

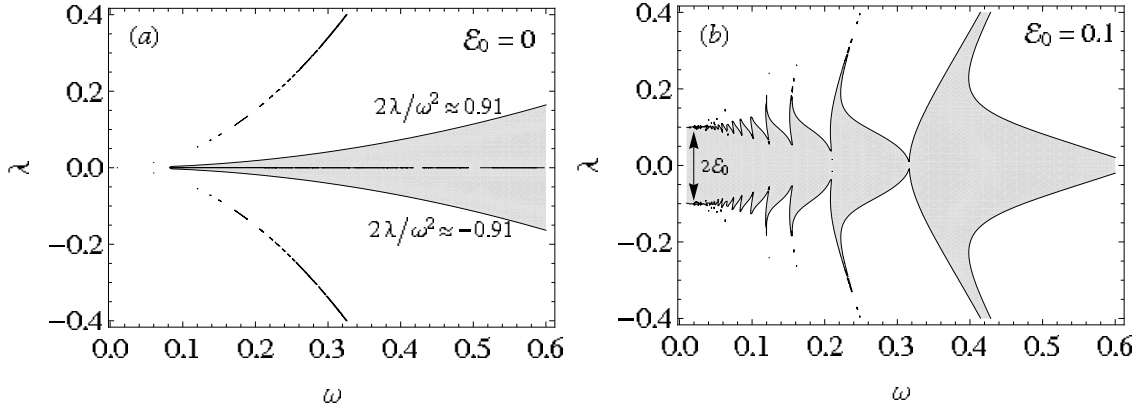


FIG. 8: The stability region for trapping state of linear solutions Eq. (17) in the  $\lambda - \omega$  plane (a) for  $\mathcal{E}_0 = 0$ , and (b) for  $\mathcal{E}_0 = 0.1$ . The shaded area stands for the stable region.

Fig. 8 gives a stability diagram of the solution Eq. (17) near the stable positions  $x^*$ , with the shaded area indicating the stable region of the trapping states. Fig. 8 shows an irregular stable parametric region of the walking determined by the lattice depth  $\lambda$  and the modulation frequency  $\omega$ , with a symmetric structure for  $\lambda$  and a fractal boundary for small  $\omega$ . Fig. 8(b) also indicates that although the symmetric gap (indicated by the arrows in Fig. 8(b)) of the stable region,  $2\mathcal{E}_0$ , in the small frequency  $\omega$  region goes to zero when  $\mathcal{E}_0 \rightarrow 0$ , the complicated structure of a stable region will not disappear in Fig. 8(a) for a real walking. This result reveals that the dynamic stability of atomic walking around antinodes in a varying lattice is very sensitive to the fluctuation of the optical field [30]. Actually the fluctuation of the lattice field will definitely make the atomic walking complicated in the small modulation frequency region. Strangely, when the modulation frequency is small, the atomic walking around antinodes can stay unstable no matter how large the depth of the lattice is. When the frequency becomes higher, the stable region will expand and the walking is more preferred to a stable motion. According to Floquet's theory, the characteristic exponent  $\mu$  of the trapping solution will be  $\lim_{\omega \rightarrow \infty} \mu(0, -2\lambda/\omega^2) = 0$ , which indicates a free atomic walking limit in a quickly varying lattice.

We should note here that the stable region of the real system Eq. (7) is not only vulnerable to the control parameters  $\lambda, \omega$  but also heavily depends on the dynamics itself, i.e., the atom's position and momentum are also key parameters for determining the stability of atomic walking [38]. The nonlinear position-dependent walking in Eq. (7) will introduce an effective part of  $\mathcal{E}_0$  to shift the atom along the lattice, which actually breaks the spatial symmetry of the lattice walking. Naturally, an increase of the atomic momentum will definitely reduce the stability region of the real trapping solution, because the heated atom will more easily escape from the trapping region. The stable region of the linear solution indicates that the atom can surely be trapped in a shallow lattice field (small  $\lambda$ ) with a higher modulation frequency  $\omega$ .

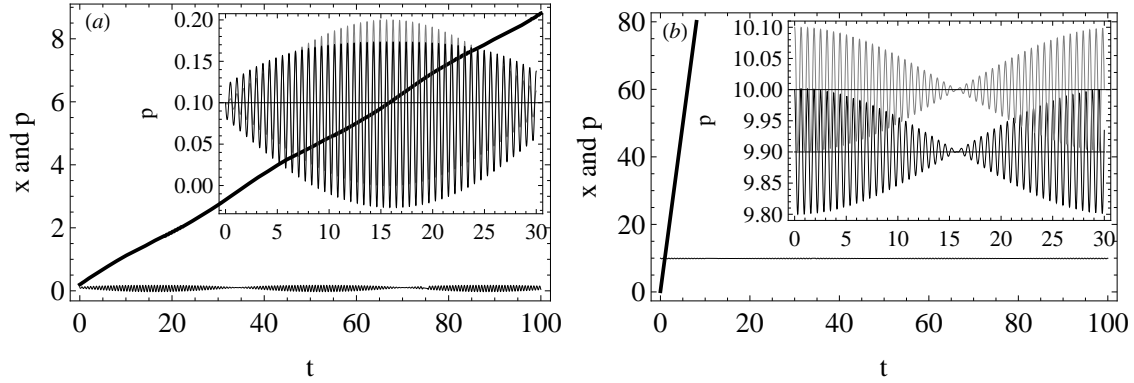


FIG. 9: The free flying of the atom (a) in a quickly varying field with  $\omega = 10$ ,  $p(0) = 0.1$ ,  $x(0) = 0.2$ ,  $\lambda = 1$ , and (b) at a high speed under parameters  $p(0) = 10$ ,  $\omega = 0.1$ ,  $x(0) = 0.2$ ,  $\lambda = 1$ . The insets are the atomic momenta zoomed in between a time interval of  $[0, 30]$  with the black lines for the strict equation and the grey ones for Eq. (19).

#### III-4. Free ballistic flying

Finally, we consider two extreme conditions: that the modulation frequency of the lattice is high ( $\omega \gg \sqrt{\lambda}$ ), and that the velocity of the atom is quick ( $p \gg 2\sqrt{\lambda}$ ). For a large modulating frequency  $\omega$ , the effective coupling constant satisfies  $\lambda \cos(\omega t) \rightarrow 0$  and the equation can be simplified to

$$\ddot{x} \approx 0, \quad \omega \gg 1, \quad (18)$$

which means a negligible influence of light on the atomic walking, and that implies a free flying of the atom in the optical lattice, i.e.,  $x(t) \approx x(0) + p(0)t$  and  $p(t) \approx p(0)$ . On the other hand, when the speed of the atom is high, the atom also feels a quick oscillation of the force with a frequency of  $p + \omega$  in one direction and  $p - \omega$  in the opposite (see Eq. (8)). Both of the above cases are displayed in Fig. 9(a) and Fig. 9(b) by direct simulations of Eq. (7), where the thick black line,  $x(t)$ , indicates a nearly free flying motion and its slope is roughly determined by the initial momentum  $p_0 \equiv p(0)$ , showing a small relative change of atomic momentum during the walking process. The enlarged figures of the momenta in the time interval  $[0, 30]$  shown by the insets of Fig. 9 demonstrate a beat oscillation of the atomic momentum around the initial value, with the average momentum satisfying  $\langle p \rangle \approx p_0$ . Therefore, the oscillation behavior can be approximately described by Eq. (8),

$$\frac{dp}{dt} = -\lambda \sin(p_0 t) \cos(\omega t),$$

and integration gives a solution

$$p(t) = p_0 + \frac{\lambda \cos[(p_0 - \omega)t]}{2(p_0 - \omega)} + \frac{\lambda \cos[(p_0 + \omega)t]}{2(p_0 + \omega)}, \quad (19)$$

which clearly reveals a beat oscillation of the momentum. Comparisons of the solution Eq. (19) (the gray lines of the insets) with the strict solution (the black lines of the insets) are depicted in Fig. 9(a) and Fig. 9(b). The simulation indicates a good agreement of Eq. (19) with the strict Eq. (7) except for some minor differences. Besides, Eq. (19) also suggests a resonance behavior of the momentum when the atomic momentum satisfies  $p_0 \approx \pm\omega$ . Under the resonant condition, Eq. (19) becomes a bad approximation because the momentum will be divergent. However, as long as the condition of  $\omega \gg \sqrt{\lambda}$  or  $p_0 \gg 2\sqrt{\lambda}$  is satisfied, the momentum enhancement by the resonant effect in a real system remains small relative to the large initial momentum, and the atom still keeps its ballistic flying under the resonance condition. However, if the initial atomic momentum is small, this resonance effect will be manifest only under small modulation frequencies (see Eq. (19)) and this resonant behavior will also be suppressed by the nonlinear character of a real walking. Therefore, in conclusion, if the modulation frequency is high and the atomic momentum is large, the atom will almost conduct a free ballistic flying with its momentum taking a beat oscillation roughly around its initial value.

#### IV. CONCLUSIONS

A single atom coupled with high-finesse cavities is a fundamental system for quantum research, and many theoretical and experimental works have been done on this system [1–5, 34–36]. Directly based on a quantum description, the quantum aspect of the dynamics are usually focused on, such as nonclassical statistics, entanglement-induced effects, and quantum information processing, which, contrarily, makes the classical contribution obscure. Yet some authors working on this system are concerned more about the transmission of the light through a cavity to detect or control the atomic dynamics [34], such as detecting atomic trapping states, or controlling atomic trajectories [40, 41]. However all the atomic motions considered above are closely involved with the internal dynamics, and the external dynamics is still mixing in atomic control. In order to investigate the external dynamics in a classical point of view, the internal variables should be decoupled or traced out. Raizen and his coworkers [42] resort to a dynamical map (periodic kicked rotator) based on a pulsed standing field to investigate the atomic dynamical behavior and find a good agreement with the classical dynamics in a noisy environment. In particular, their experiment which studies the motion of cold cesium atoms in an amplitude-modulated standing wave of light [29, 30] has a very close relation to our study in this paper. However, we use a simple classical model under a resonant condition and find a more rich dynamic behavior of one atom in the optical lattice beyond a direct influence of the internal quantum dynamics.

For the fluctuating environment of the cavity mode, trapping a single atom in the cavity for a long time has turned out to be difficult. Therefore, sensitivity of the atomic motion to field modulation is a key problem for a practical one-atom control [30]. In this paper, we closely consider the classical walking of an atom in a field-controlled standing wave and revealed a diverse dynamic region of atomic motion. In the parametric region of lower modulation frequency, an oscillation with classical random jumping is found for a cold

atom. With an increase of frequency, random atomic motion, chaotic transportation, and the quasi-periodic trapping state appear. If the modulation frequency is high or the velocity of the atom in the lattice is large, the atom will exhibit a ballistic fly with a momentum beating the oscillation. The study of dynamic stability shows that the transition between these dynamical regimes is irregularly determined not only by the lattice field but also by the position and momentum of the atom. Our results indicate a wide parametric region of unstable walking and a susceptibility of stable motion to the field fluctuations of amplitude and frequency as well as to the motion itself. Therefore, this work gives a rich clue for atomic control in a cavity and also provides a useful statistical insight into the dynamical behavior of an atom in a periodically varying lattice.

### Acknowledgements

This work is supported by the Shaanxi Provincial Natural Science Foundation (No. SJ08A12) and the National Science Foundation Project (No. 10875076).

### APPENDIX A: THE DERIVATION OF EQ. (4)

The dynamics of an atom in a certain field can be manipulated by different configurations of  $\mathbf{E}(\mathbf{r}, t)$  according to the Hamiltonian of Eq. (2). A standing wave, generated by an interference of two quasi-monochromatic fields with an envelope,  $\mathcal{E}(\mathbf{r}, t)$ , and the polarization,  $\mathbf{e}_\lambda$ , propagating in opposite directions, has the form

$$\begin{aligned}\mathbf{E}(\mathbf{r}, t) &= \frac{1}{2} \mathbf{e}_\lambda \mathcal{E}(\mathbf{r}, t) [\cos(\nu t + \mathbf{k} \cdot \mathbf{r}) + \cos(\nu t - \mathbf{k} \cdot \mathbf{r})] \\ &= \mathbf{e}_\lambda \mathcal{E}(\mathbf{r}, t) \cos(\mathbf{k} \cdot \mathbf{r}) \cos(\nu t),\end{aligned}$$

where  $\nu$  is the carrier frequency and the slowly varying temporal envelope,  $\mathcal{E}(\mathbf{r}, t)$ , can be controlled in the experiment by changing the amplitude of the input field. If we stabilize the phase of the field in a linear cavity along the  $x$  axis, the Hamiltonian of Eq. (3) will be obtained. More generally, we can write down the Schrödinger equation for the standing wave as

$$i\hbar \frac{\partial}{\partial t} \Psi(\mathbf{r}, t) = \left[ \frac{\hat{p}^2}{2m} + \hat{H}_a - \Omega(\mathbf{r}, t) \cos(\nu t) \right] \psi(\mathbf{r}, t),$$

where

$$\Omega(\mathbf{r}, t) = \hat{\mathbf{d}} \cdot \mathbf{e}_\lambda \mathcal{E}(\mathbf{r}, t) \cos(\mathbf{k} \cdot \mathbf{r}),$$

and  $\hat{H}_a$  denotes the energy of the internal state: on ground state  $|1\rangle$  with energy  $\epsilon_1$  and on excited state  $|2\rangle$  with energy  $\epsilon_2$ . In real space, the atomic wavefunction can be written by a two-component form of

$$\Psi(\mathbf{r}, t) = \varphi_1(\mathbf{r}, t) e^{-i\epsilon_1 t/\hbar} |1\rangle + \varphi_2(\mathbf{r}, t) e^{-i\epsilon_2 t/\hbar} |2\rangle.$$

Under the rotating wave approximation, the Schrödinger equation for the two-component wave function is

$$\frac{\partial}{\partial t} \begin{pmatrix} \varphi_1 \\ \varphi_2 \end{pmatrix} = i \begin{pmatrix} \frac{\hbar}{2m} \nabla^2 & \Omega_R(\mathbf{r}, t) e^{-i\delta t} \\ \Omega_R(\mathbf{r}, t) e^{i\delta t} & \frac{\hbar}{2m} \nabla^2 \end{pmatrix} \begin{pmatrix} \varphi_1 \\ \varphi_2 \end{pmatrix},$$

where the detuning frequency is  $\delta = \omega_0 - \nu$  and the transition frequency is  $\omega_0 = (\epsilon_2 - \epsilon_1) / \hbar$ . The Rabi frequency is defined by

$$\Omega_R(\mathbf{r}, t) = \frac{\Omega(\mathbf{r}, t)}{2\hbar} = \frac{\hat{\mathbf{d}} \cdot \mathbf{e}_\lambda}{2\hbar} \mathcal{E}(\mathbf{r}, t) \cos(\mathbf{k} \cdot \mathbf{r}).$$

In the experiment, the carrier frequency  $\nu$  is adjusted to the transition frequency  $\omega_0$  (resonance  $\delta = 0$ ), then

$$i\hbar \frac{\partial}{\partial t} \begin{pmatrix} \varphi_1 \\ \varphi_2 \end{pmatrix} = \begin{pmatrix} -\frac{\hbar^2}{2m} \nabla^2 & -\hbar\Omega_R(\mathbf{r}, t) \\ -\hbar\Omega_R(\mathbf{r}, t) & -\frac{\hbar^2}{2m} \nabla^2 \end{pmatrix} \begin{pmatrix} \varphi_1 \\ \varphi_2 \end{pmatrix}.$$

In this case the above equation can be decoupled by introducing [43]

$$\psi_+(\mathbf{r}, t) = \frac{1}{\sqrt{2}} [\varphi_1(\mathbf{r}, t) + \varphi_2(\mathbf{r}, t)], \quad \psi_-(\mathbf{r}, t) = \frac{1}{\sqrt{2}} [\varphi_1(\mathbf{r}, t) - \varphi_2(\mathbf{r}, t)],$$

with the equations

$$i\hbar \frac{\partial}{\partial t} \psi_+ = -\frac{\hbar^2}{2m} \nabla^2 \psi_+ - \hbar\Omega_R(\mathbf{r}, t) \psi_+, \quad i\hbar \frac{\partial}{\partial t} \psi_- = -\frac{\hbar^2}{2m} \nabla^2 \psi_- + \hbar\Omega_R(\mathbf{r}, t) \psi_-.$$

The above equations for the wave functions  $\psi_\pm(\mathbf{r}, t)$  indicates that the atom in any state will feel two different potentials:

$$V_\pm(\mathbf{r}, t) = \mp \hbar\Omega_R(\mathbf{r}, t) = \mp \frac{\hat{\mathbf{d}} \cdot \mathbf{e}_\lambda}{2} \mathcal{E}(\mathbf{r}, t) \cos(\mathbf{k} \cdot \mathbf{r}).$$

If the envelope function of the field is controlled by (amplitude modulation field)

$$\mathcal{E}(\mathbf{r}, t) = g_0 \cos(\chi t),$$

the effective potential will be

$$V(\mathbf{r}, t) = \mp g_0 \frac{\hat{\mathbf{d}} \cdot \mathbf{e}_\lambda}{2} \cos(\chi t) \cos(\mathbf{k} \cdot \mathbf{r}) \equiv \hbar\lambda \cos(\chi t) \cos(\mathbf{k} \cdot \mathbf{r}).$$

For a linear cavity, the effective potential we pick up to consider is

$$V(x, t) = \hbar\lambda \cos(\chi t) \cos(kx),$$

where  $\lambda$  is the effective coupling parameter and  $\chi$  is the modulation frequency of the field amplitude.

## References

\* Electronic address: [zhanglincn@snnu.edu.cn](mailto:zhanglincn@snnu.edu.cn)

- [1] I. Teper, Yu-Ju Lin, and V. Vuletić, *Phys. Rev. Lett.* **97**, 023002 (2006).
- [2] A. Stibor *et al.*, *New J. Phys.* **12**, 065034 (2010).
- [3] J. Ye, D. W. Vernooy, and H. J. Kimble, *Phys. Rev. Lett.* **83**, 4987 (1999).
- [4] S. Kuhr *et al.*, *Science* **293**, 278 (2001).
- [5] T. Wilk, S. C. Webster, A. Kuhn, and G. Rempe, *Science* **317**, 488 (2007).
- [6] C. Monroe, *Nature* **416**, 238 (2002).
- [7] R. Arun, O. Cohen, and I. Sh. Averbukh, *Phys. Rev. A* **81**, 063809 (2010).
- [8] S. R. Wilkinson, C. F. Bharucha, K. W. Madison, Q. Niu, and M. G. Raizen, *Phys. Rev. Lett.* **76**, 4512 (1996).
- [9] M. Karski *et al.*, *Science* **325**, 174 (2009).
- [10] J. Jooa, P. L. Knight, and J. K. Pachos, *J. Mod. Opt.* **54**, 1627 (2007).
- [11] S. Nie and S. R. Emory, *Science* **275**, 1102 (1997).
- [12] D. E. Chang *et al.*, *Phys. Rev. Lett.* **103**, 123004 (2009).
- [13] F. L. Moore, J. C. Robinson, C. F. Bharucha, B. Sundaram, and M. G. Raizen, *Phys. Rev. Lett.* **75**, 4598 (1995).
- [14] A. C. Doherty, A. S. Parkins, S. M. Tan, and D. F. Walls, *Phys. Rev. A* **56**, 833 (1997).
- [15] P. Horak, G. Hechenblaikner, K. M. Gheri, H. Stecher, and H. Ritsch, *Phys. Rev. Lett.* **79**, 4974 (1997).
- [16] R. Graham, M. Schlautmann, and P. Zoller, *Phys. Rev. A* **45**, R19 (1992).
- [17] In a real atomic scale experiment, one atom can be traced and detected with a high resolution beyond the Heisenberg uncertainty principle.
- [18] D. M. Meekhof, C. Monroe, B. E. King, W. M. Itano, and D. J. Wineland, *Phys. Rev. Lett.* **76**, 1796 (1996).
- [19] V. Yu. Argonov and S. V. Prants, *Phys. Rev. A* **75**, 063428 (2007).
- [20] V. Yu. Argonov and S. V. Prants, *Phys. Rev. A* **78**, 043413 (2008).
- [21] S. V. Prants, *JETP Lett.* **75**, 777 (2007).
- [22] S. V. Prants, M. Edelman, and G. M. Zaslavsky, *Phys. Rev. E* **66**, 046222 (2002).
- [23] S. V. Prants and V. Yu. Sirotkin, *Phys. Rev. A* **64**, 033412 (2001).
- [24] F. Toscano, and D. A. Wisniacki, *Phys. Rev. E* **74**, 056208 (2006).
- [25] C. Gerry and P. Knight, *Introductory Quantum Optics*, Cambridge University Press, (Cambridge, 2005), Chap. 4.
- [26] A. R. Kolovsky, *Quantum chaos: double resonance model and its physical applications*, Lecture Notes in Physics **457**, 461 (1995).
- [27] F. Saif, *Phys. Rep.* **419**, 207 (2005).
- [28] P. L. Gould, G. A. Ruff, and D. E. Pritchard, *Phys. Rev. Lett.* **56**, 827 (1986).
- [29] D. A. Steck, W. H. Oskay, and M. G. Raizen, *Science* **293** 274 (2001).
- [30] D. A. Steck, W. H. Oskay, and M. G. Raizen, *Phys. Rev. Lett.* **88**, 120406 (2002).
- [31] F. L. Moore, J. C. Robinson, C. Bharucha, P. E. Williams, and M. G. Raizen, *Phys. Rev. Lett.* **73**, 2974 (1994).
- [32] D. B. Monteoliva, B. Mirbach, and H. J. Korsch, *Phys. Rev. A* **57**, 746 (1998).
- [33] L. E. Reichl, *The Transition to Chaos: Conservative Classical Systems and Quantum Manifestations*, 2nd ed, (Springer, NewYork, 2004).
- [34] P. Münstermann, T. Fischer, P. Maunz, P. W. H. Pinkse, and G. Rempe, *Phys. Rev. Lett.* **82**, 3791 (1999).
- [35] J. McKeever *et al.*, *Phys. Rev. Lett.* **90**, 133602 (2003).

- [36] P. Domokos and H. Ritsch, *Phys. Rev. Lett.* **89**, 253003 (2002).
- [37] S. V. Prants and M. Yu. Uleysky, *Phys. Lett. A* **309**, 357 (2003).
- [38] G. Teschl, *Ordinary Differential Equations and Dynamical Systems*, Lecture Notes, <http://www.mat.univie.ac.at/gerald>.
- [39] A. Mouchet, C. Miniatura, R. Kaiser, B. Grémaud, and D. Delande, *Phys. Rev. E* **60**, 016221 (2001).
- [40] C. J. Hood, T. W. Lynn, A. C. Doherty, A. S. Parkins, and H. J. Kimble, *Science* **287**, 1447 (2000).
- [41] T. W. Lynn, K. Birnbaum, and H. J. Kimble, *J. Opt. B: Quantum Semiclass. Opt.* **7**, S215 (2005).
- [42] D. A. Steck, V. Milner, W. H. Oskay, and M. G. Raizen, *Phys. Rev. E* **62**, 3461 (2000).
- [43] R. J. Cook, *Phys. Rev. Lett.* **41**, 1788 (1978).